Robotica (2025), **43**, pp. 242–255
doi:10.1017/S0263574724001826

CAMBRIDGE UNIVERSITY PRESS

RESEARCH ARTICLE

Nuclear bilateral telerobotic systems: performance comparison and future implications

Harun Tugal[1], Fumiaki Abe[2], Masaki Sakamoto[2], Shu Shirai[2], Ipek Caliskanelli[1], Wenxing Liu[1], Hector Marin-Reyes[1], Kaiqiang Zhang[1] and Robert Skilton[1]

[1]UK Atomic Energy Authority (UKAEA), Remote Applications in Challenging Environments (RACE), Culham Campus, Abingdon, UK
[2]Tokyo Electric Power Company (TEPCO) and secondees at RACE/UKAEA, Culham Campus, Abingdon, UK
Corresponding author: Harun Tugal; Email: harun.tugal@ukaea.uk

Received: 10 June 2024; **Revised:** 12 September 2024; **Accepted:** 26 September 2024;
First published online: 29 October 2024

Keywords: Bilateral teleoperation; performance measurements; standardization

Abstract

This article presents a comprehensive evaluation of two nuclear-rated bilateral telerobotic systems, Telbot and Dexter, focusing on critical performance metrics such as effort transparency, stiffness, and backdrivability. Despite the absence of standardized evaluation methodologies for these systems, this study identifies key gaps by experimentally assessing the quantitative performance of both systems under controlled conditions. The results reveal that Telbot exhibits higher stiffness, but at the cost of greater effort transmission, whereas Dexter offers smoother backdrivability. Furthermore, positional discrepancies were observed during the tests, particularly in nonlinear positional displacements. These findings highlight the need for standardized evaluation methods, contributing to the development, manufacturing, and procurement processes of future bilateral telerobotic systems.

1. Introduction

Bilateral telerobotic systems have fundamentally transformed the way humans interact with distant objects. These kinesthetically coupled systems facilitate an operator in receiving haptic feedback from a local device as the remote manipulator engages with its environment. This additional feedback channel enhances the operator's ability to perform delicate tasks with higher precision and situational awareness, significantly reducing the time needed to complete tasks (e.g., see refs. [1, 2]). Consequently, telerobotic systems have become indispensable in critical sectors such as nuclear facilities (e.g., material handling, waste disposal, or fusion power plant maintenance), space and underwater explorations, military operations, and telesurgery, underlining their importance through decades of extensive research [3, 4].

Two critical performance metrics in these systems are effort transparency—the ability of the system to accurately transmit forces and torques between the local and remote manipulators—and back drivability, which refers to the system's capability to allow the local manipulator to be controlled through movements applied at the remote manipulator. Both are essential for ensuring that the operator experiences realistic and responsive interactions during teleoperation.

Central to the design of bilateral teleoperation systems is achieving absolute stability, especially given the highly uncertain and variable dynamics of human arm and environmental interactions [5]. Balancing stability with performance presents a major design challenge, making it a focal point of discussion in the field [6, 7]. Historically, performance evaluations have primarily assessed position tracking and force reflection. However, these assessments have mostly been limited to single-degree-of-freedom (DoF) systems, which are inadequate for evaluating multi-DoF systems [8].

© The Author(s), 2024. Published by Cambridge University Press.

https://doi.org/10.1017/S0263574724001826 Published online by Cambridge University Press

Recent research has introduced advanced metrics and techniques for evaluating telerobotic systems. For example, a cloud-based approach for nondestructive material characterization [9] could enhance real-time inspection in telerobotic environments. Similarly, methods for optimizing energy consumption in wireless sensor networks [10] could improve data transmission and control in systems relying on wireless communication. These efforts have contributed to the ongoing development of robust, efficient telerobotic systems.

However, despite well-established evaluation methodologies for industrial manipulators and collaborative robots (e.g., ISO 9283:1998, ISO/TS 150:2016), a standardized approach for assessing multi-DoF bilateral telerobotic systems remains absent [11]. This lack of standardization is particularly evident in evaluating critical performance criteria such as stiffness [8] and backdrivability across different mechanical design philosophies [12]. The absence of a standardized evaluation framework highlights the need for developing methodologies that can experimentally assess these critical performance aspects.

Previous studies on bilateral telerobotic systems primarily focused on bandwidth and frequency response, which are difficult to quantify or measure [13, 14]. Early performance measures, such as peak force, peak acceleration, and impedance characteristics, were introduced by Hayward et al. [15]. Later studies, such as those by Cavusoglu [16] and Taati [17], identified specific performance measures for haptic interfaces, while backdrivability was experimentally evaluated in ref. [18] against communication delays. A comprehensive review of haptic system evaluations, covering both qualitative and quantitative aspects, was detailed in ref. [11].

Effort transparency remains a key performance metric for haptic systems, with various control methodologies proposed to enhance it [19]. In an ideal bilateral telerobotic system, the force/torque applied at the local end would be seamlessly transmitted to the remote end [20]. Achieving perfect transparency is difficult due to stability constraints, as well as hysteresis introduced by system dynamics.

Also, the ratio between an applied force and the resulting displacement is important in both the local and remote manipulators which is known as stiffness (also referred to as lost motion and rigidity) [21–24]. Typically, high degrees-of-freedom bilateral telerobotic setups are position-based systems; force reflection on the local side is achieved by comparing the pose of the local and remote manipulators [25]. Therefore, stiffness is a critical criterion, as a low value might result in a *spongy* feeling when the remote manipulator interacts with a stiff object [26, 27].

Backdrivability refers to a system's capability to operate in reverse, allowing manipulation of the local arm by driving the remote arm [28]. In position-based bilateral telerobotic systems, where the remote joint angle is controlled by the local joint angles, backdrivability is also essential for generating positional discrepancies that contribute to the sensation of effort at the local side, ultimately influencing overall transparency [18, 29]. Additionally, highly backdrivable systems offer substantial operational flexibility, reducing the risk of damage during contact with harsh environments and providing a safety margin [28]. Therefore, assessing system performance includes considering its backdrivability as a valuable indicator.

This study aims to contribute to the broader efforts of standardizing evaluation methodologies for bilateral telerobotic systems, which will enhance consistency in development, manufacturing, and procurement processes. Here, we experimentally evaluate quantitative performance measures—such as effort transparency, stiffness, and back drivability—of two nuclear-rated bilateral telerobotic systems known as Telbot and Dexter. Alongside presenting performance results, the paper comprehensively outlines test procedures, measurement methods, and conditions. This approach aims to establish accepted sets of performance measures and benchmarks, facilitating comparison between different designs while potentially guiding future developments.

2. Methods

2.1. Notations

Bold lower-case letters, $\boldsymbol{x}$, represent the column vectors, nonbold upper case-letters, X, denote matrices, nonbold lower-case letters, x, represent single variables, and $^\top$ denotes the transpose. The transformation

https://doi.org/10.1017/S0263574724001826 Published online by Cambridge University Press



Figure 1. *Telbot bilateral telerobotic system: on the left, the local station, and on the right, the remote side, both featuring kinematically similar configurations.*



Figure 2. *Dexter bilateral telerobotic system: The left depicts the local side, while the right shows the remote side, both sharing kinematically identical configurations.*

from a vector to a skew-symmetric matrix is denoted by $[\,]_\times$ operator. The identify matrix is denoted as I.

2.2. Experimental setup

The experiment utilized two advanced robotic systems, the Telbot and Dexter, both dual-arm bilateral teleoperation systems with distinct mechanical design philosophies. These systems consist of local and remote manipulators designed for precise teleoperation tasks. The details of the systems' configurations are shown in Figures 1 and 2.

The Telbot and Dexter systems are bilateral teleoperation setups, each driven by gears and tendons, respectively. Both systems feature local and remote manipulators. Excluding the gripper, Telbot's local manipulator offers seven degrees of freedom and is capable of carrying up to 20 kg at the end-effector. Dexter's local manipulator provides six degrees of freedom with a payload capacity of 10 kg. Remote control for both systems is facilitated through their local manipulators: in Telbot, the remote arm has a kinematically similar structure, whereas Dexter's remote arm is identical to its local counterpart.

Telbot's remote arm uses a mechanism where the motion is transmitted from base-located motors to the end-effector via concentric tubes and bevel gears, allowing for unrestricted rotation across all axes. This design provides a positioning accuracy of 0.1 mm for repeated movements [30]. Conversely, Dexter's lightweight manipulators transmit motion through tendons, from base-located motors to the handle or end-effector. Both local and remote arms of Dexter possess six degrees of freedom and are operated manually by human users.

To measure transmitted effort, ATI Gamma Force/Torque (FT) sensors (calibrated with SI 330-30) were installed close to the handle point on the local side and the tool center point (TCP) on the remote

https://doi.org/10.1017/S0263574724001826 Published online by Cambridge University Press

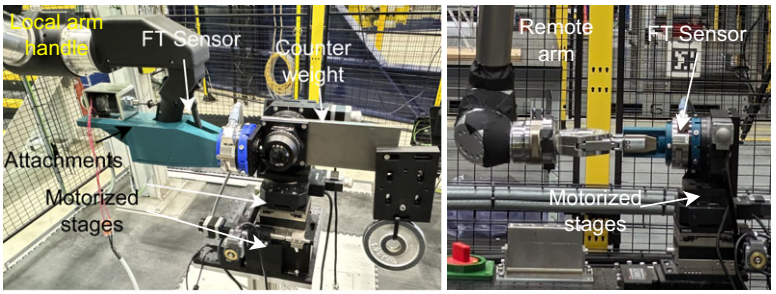


Figure 3. *Experimental setup consisting of Telbot local and remote arms, 2 FT sensors, translational and rotational stages.*

side. These sensors captured the transmitted effort between the operator and the manipulators (and between manipulator and the environment) during the experiment.

These telerobotic interfaces are designed for operator use. However, human-in-the-loop experiments can be highly variable and difficult to replicate. To introduce consistent positional disturbances, we used high-resolution multiaxis motorized stages that could be controlled remotely. These stages were mounted at the operational points of both the local and remote manipulators. For added safety, the telerobotic systems were activated and deactivated remotely. Telbot's enabling switch, located on the handle, was controlled by a solenoid system. This remote activation feature complemented existing safety barriers and external emergency switches.

To induce perturbations in both local and remote manipulators along the x, y, z, roll (r_x), pitch (r_y), and yaw (r_z) directions, multiple motorized stages were assembled, as shown in Figure 3. When perturbing the local manipulator, an FT sensor was mounted at the tip of the translational and rotational stages and connected to the tip of the local manipulator using a custom attachment tools.

Typically, a displacement exists between the sensor frame's origin and the main contact point's origin (e.g., the handle point at the local or the tool center point at the remote sides) due to the attachment tools. This displacement affects the transformation of forces and torques (FT) from the sensor frame to the contact point. In that case, the force/torque vector at the handle, $\boldsymbol{f}_h$, is related to the sensor frame measurement, $\boldsymbol{f}_{tcp}$, as

$$\boldsymbol{f}_h = \begin{bmatrix} \mathrm{I} & 0 \\ [\boldsymbol{p}_c^s]_\times & \mathrm{I} \end{bmatrix} \boldsymbol{f}_s,$$

where $\boldsymbol{f}_s = \begin{bmatrix} f_s^x & f_s^y & f_s^z & \tau_s^x & \tau_s^y & \tau_s^z \end{bmatrix}^\top$ is the FT exerted by the handle (end-effector) on its environment, derived from the FT sensor reading by removing the efforts generated by the weight of the tool (and then taking the negative as the force sensor measurement is the actual force applied by the end-effector on the environment where in bilateral system we are interested how much environmental force transmitted to the human/operator hand). The origin of the sensor frame (s) with respect to the contact point position in the sensor frame is denoted by the position vector $\boldsymbol{p}_c^s$. This equation allows us to transform the sensor's FT readings to the actual point of interest, compensating for any displacement caused by tool attachments. All reported efforts refer to those measured at the handle and tool-centre points in the depicted base frame.

2.3. Experimental procedures

2.3.1. Testing conditions

In both systems, the operator could adjust the level of haptic feedback through the human–machine interface (HMI). For the Telbot system, the feedback was set to 100% (full force/torque feedback), while

https://doi.org/10.1017/S0263574724001826 Published online by Cambridge University Press

for Dexter, the tests were conducted using a 1.5 scale ratio for the force feedback, which is the default setting recommended by the manufacturer. This scale ratio reduce the perceived force by 1.5 times, providing the operator with sufficient sensitivity to remote manipulations, facilitating finer control.

The performance measures in these systems are inherently dependent on the operating point. To ensure consistency across trials, the remote manipulator in both systems was positioned near the center of the operational workspace during the experiments. For example, in Dexter, this meant that each joint was positioned approximately midway between its upper and lower limits, which represents the normal operating posture of the system.

Prior to each test, all systems were powered on for 30–45 minutes to allow the equipment to stabilize at its nominal operating temperature. This step is critical, particularly for mitigating sensor output drift—especially in force/torque (FT) sensors, which are susceptible to drift over time due to fluctuations in temperature and gage excitation voltage. By allowing the system to reach thermal equilibrium, we reduced the risk of inaccurate measurements. To further counteract sensor drift, the FT sensors were biased before each testing cycle in accordance with the manufacturer's guidelines. Although biasing does not eliminate drift entirely, it effectively reduces the cumulative effect, ensuring that sensor outputs start from zero at the beginning of each cycle.

To minimize the impact of thermal drift during extended testing periods, we used 3D-printed plastic tools as attachments, which offered better thermal stability compared to metal components.

The temperature of the ambient environment during the tests was $(20 \pm 2.5)^{\circ}$C, in line with the industrial manipulator performance measure standard [31]. Since the measurement took place in the premises that were not air-conditioned, it was not possible to secure the temperature $(20 \pm 2.0)^{\circ}$C. The tests were conducted in the allowed temperature range specified by the manufacturer of the Telbot and Dexter: (10°C to 40°C), FT sensor ((0°C to 70°C)).

In addition to reporting the standard deviations from multiple measurements, we conducted a comprehensive review of potential sources of error that could have impacted the experimental results. All force/torque sensors were calibrated by the manufacturers using appropriate calibration ranges to ensure accuracy. The mechanical rigidity of the system was thoroughly examined, and any potential deflections in the tools and attachment links were minimized through adjustments made prior to the experiments.

2.3.2. Initialization and data collection protocol

A slowly increasing and decreasing ramp input is applied to the motorized stages, allowing for the generation of an output versus input force graph. This curve, also known as the transparency curve of a device, illustrates the linearity of force transmission. From this graph, various output force limits can be extracted, such as the maximum continuous force (due to saturation), dead zone (attributed to stiction and Coulomb friction), and hysteresis (resulting from backlash, loose components, and friction). The slope of the linear portion of the calibration curve, known as sensitivity, reflects the change in output for a unit change in input, with higher sensitivity being desirable for any bilateral teleoperation system. The limit of the dead zone indicates the minimum force that a haptic device can generate [11], also referred to as the static friction breakaway (SFB) force. This term denotes the minimum amount of force or torque required at the local side to initiate the transmission of effort to the remote side.

Tests were conducted in six directions within the Cartesian frame. In each test, the end effector of the local arm (the handle) was displaced with a velocity of 0.01 mms^{-1} (0.01° $s^{-1}0$) at linear (orientation) frames, reaching a maximum of 4 mm (2°) in 10 cycles, see Table I. In each direction, two sets of experiments were conducted–one in the positive direction and one in the negative direction.

In order to test effort transparency of the bilateral teleoperation systems, FT sensors were mounted to the local arm handle point and remote arm TCP, also motorized stages were mounted to the local arm as seen in Figure 3. The diagram illustrating the overall test setup is presented in Figure 4.

The stiffness tests were conducted with FT sensors and motorized stages mounted on the local manipulators. The remote manipulator grasped a stiff plate, and in Dexter, remote manipulators' brakes were engaged. and in the Telbot, the grippers were mechanically locked to prevent any undesirable

https://doi.org/10.1017/S0263574724001826 Published online by Cambridge University Press

Table I. *Commanded displacements and velocities recorded during various tests.*

	Translation (Orientation)	
Performance	**Max. Displacement**	**Velocity**
Effort Tr.	4 mm (2°)	0.01 mm s^{-1} (0.01° s^{-1})
Stiffness	50 mm (20°)	0.1 mm s^{-1} (0.1° s^{-1})
Back dr.	50 mm	1 mm s^{-1}

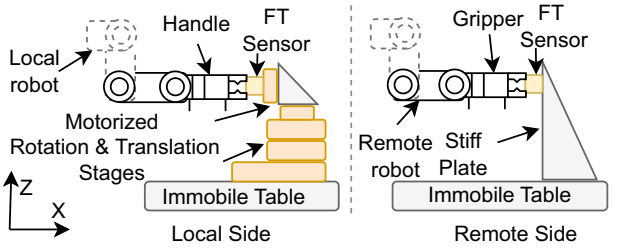


Figure 4. *In the transparency setup, a small input is applied to the local device, and the response is recorded on both sides. During the effort transparency test, measurements from the FT sensor are taken into consideration.*

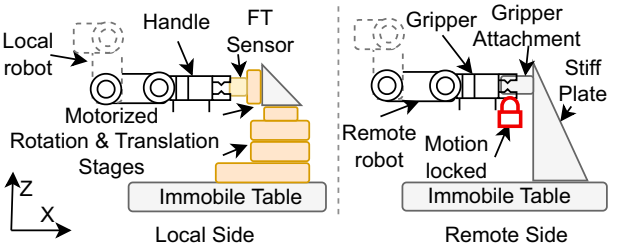


Figure 5. *In the stiffness test setup, input is applied to the local device, while the motion is constrained in the remote device.*

displacement at the TCP. Positional displacement is applied to the local arms by gradually increasing the ramp input to the motorized stages. The diagram illustrating the overall test setup is presented in Figure 5.

Stiffness is a fundamental concept in both mechanics and control systems, describing how much an object resists deformation in response to applied forces or torques. Using Hooke's law, stiffness is defined as a linear relationship between the applied force/torque and the corresponding displacement:

$$\boldsymbol{f} = K\Delta\boldsymbol{p},$$

where $K \in \mathbb{R}^{6\times6}$ is symmetric and positive definite stiffness matrix, representing the system's resistance to deflection in both translational and rotational directions. The displacement vector is denoted as $\Delta\boldsymbol{p} = \left[\Delta p^x \ \Delta p^y \ \Delta p^z \ \Delta\theta^x \ \Delta\theta^y \ \Delta\theta^z\right]^\top$, where Δp and $\Delta\theta$ represent linear and angular displacements, respectively. And $\boldsymbol{f} = \left[f^x \ f^y \ f^z \ \tau^x \ \tau^y \ \tau^z\right]^\top$ is the effort vector [32, 19].

This equation is crucial for analysing the system's stiffness behavior, especially in the context of bilateral teleoperation, where stiffness needs to be carefully controlled to ensure both stability and transparency.

During the backdrivability test, the local manipulator is allowed to move freely, while positional displacement is applied at the remote end. Ideally, the local position should track the remote's position

https://doi.org/10.1017/S0263574724001826 Published online by Cambridge University Press

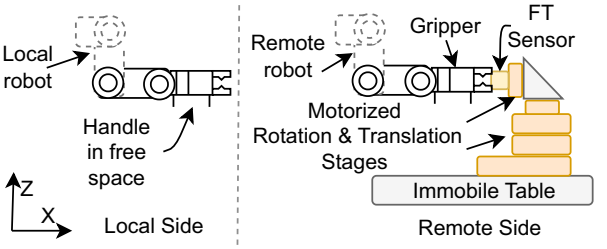


Figure 6. *In the back drivability setup, input is only applied to the remote device, and the response is recorded on both sides.*

within a stability boundary. Thus, motorized stages were only mounted on the remote manipulator end-effector, and the actuators were operated while the local arm was in free space. The diagram illustrating the overall test setup is presented in Figure 6.

3. Main results

We evaluated the transparency, stiffness, and backdrivability of telerobotic systems. Statistical analyses were conducted to determine if there were significant differences between left and right hands or among the manipulators. Normality tests confirmed that all data groups followed a normal distribution at a significance level of 0.05.

To assess effort transparency, we used Welch's *t*-test (implemented in Matlab using *ttest2()*). A significance threshold of 0.05 was maintained for all statistical tests in this study.

3.1. Effort transparency results

In dynamic tasks, one critical parameter is the effort transmission point, often referred to as the SFB point. This point indicates where static friction is overcome, allowing movement to occur. It can be identified by the peak in the derivative of the remote force/torque vector (i.e., yank) [33] as:

$$y_{sfb} = \max_i \frac{d\,|f^i_{tcp}\,|}{dt}$$

where f^i_{tcp} is the force/torque component in the i-th operational space direction. The derivative $\frac{d|f^i_{tcp}|}{dt}$ captures the rate of change of the force/torque, with the maximum point indicating the SFB.

To minimize the influence of sensor noise and ensure accurate identification of the breakaway point, a Savitzky-Golay filter is applied to smooth the force/torque data. This filtering technique preserves the significant features of the signal while reducing noise, enabling precise identification of the first effort transmission point. Figure 7 illustrates local and remote forces and position of the local manipulator (i.e., motorized stages) while conducting force transparency test with Telbot left-hand-side arm in z-direction.

The estimated SFB FT for the Telbot manipulators is given in Table II. In the left-hand side (LHS), the system demonstrated force transmission starting values ranging from 1.8163 N (in the x-direction) to 4.5536 N (in the z-direction). Additionally, the LHS exhibited moment transmission values, with r_x, r_y, and r_z values at 0.6772 N m, 1.1361 N m, and 0.7755 N m, respectively. On the right-hand side (RHS), the force sensitivity ranged from 1.1461 N (in the y-direction) to 2.0707 N (in the z-direction), while the moment transmission starting values was notable in r_x (0.5745 N m), r_y (0.0027 N m, that is a significantly lower value due to estimating points only close to/similar to the starting points), and r_z (0.4234 N m). These findings provide a comprehensive understanding of the telerobotic system's operator's sensitivity to external forces and moments across different axes.

https://doi.org/10.1017/S0263574724001826 Published online by Cambridge University Press

Table II. *Telbot and Dexter SFB forces/torques (y_{sfb}).*

	Telbot		Dexter	
Direction	**LHS**	**RHS**	**LHS**	**RHS**
x (N)	1.8163 (±0.96)	1.8825 (±0.84)	0.8403 (±0.59)	1.3403 (±0.91)
y (N)	1.8447 (±1.57)	1.1461 (±0.73)	0.7951 (±0.51)	0.2392 (±0.60)
z (N)	4.5536 (±1.69)	2.0707 (±1.7)	0.4812 (±0.47)	1.6475 (±0.69)
r_x (N m)	0.6772 (±0.23)	0.5745 (±0.17)	0.1121 (±0.04)	0.1049 (±0.03)
r_y (N m)	1.1361 (±0.48)	0.0027 (±0.002)	0.0394 (±0.07)	0.0058 (±0.003)
r_z (N m)	0.7755 (±0.26)	0.4234 (±0.39)	0.7393 (±0.15)	0.0128 (±0.01)
Average				
Translation (N)	2.7382	1.6998	0.7055	1.0757
Rotation (N m)	0.8629	0.3335	0.2969	0.0411

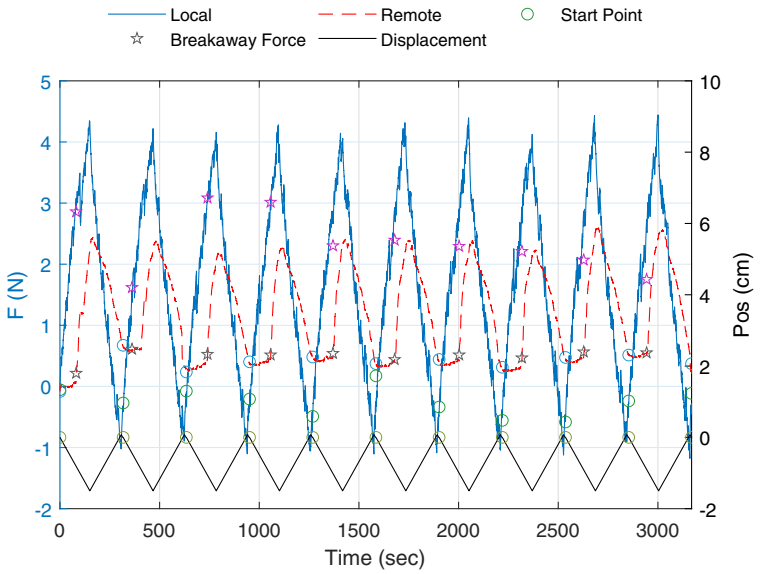


Figure 7. *Force transparency test with LHS Telbot manipulator in z-direction.*

Although the Telbot LHS and RHS arms are identical, their friction compensation parameters are tuned differently in the low-level controller.[1] This leads to varied outcomes, with the LHS arm typically requiring higher efforts to initiate transmission to the remote side across multiple axes. The analyses indicate a statistically significant difference ($p = 0.000364$) in translational SFB FT between Telbot's LHS and RHS.

The estimated SFB FT for the Dexter manipulators is provided in Table II as well. The lightweight, low-inertia mechanical design of both the local and remote manipulators, combined with the tendon driving mechanism, influences the estimated results. As a result, relatively low effort is required in both the LHS and RHS Dexter arms to initiate the transmission of effort to the remote side.

The Telbot system exhibits higher SFB forces in all translational directions compared to the Dexter system ($p = 0.0001$). Specifically, the z-direction in Telbot shows significant force resistance, with the LHS recording a breakaway force of 4.5536 N and the RHS at 2.0707 N, whereas Dexter's corresponding

[1] Confirmed by the manufacturer.

https://doi.org/10.1017/S0263574724001826 Published online by Cambridge University Press

Table III. *Stiffness (N m^{-1} – N m rad^{-1}) of the Telbot system in both arms.*

	Left Hand Side (LHS)			Right Hand Side (RHS)		
Direction	**Displacement (mm-deg)**	**Effort (N-N m)**	**Stiffness**	**Displacement (mm-deg)**	**Effort (N-N m)**	**Stiffness**
x	31.4136	69.5363	2213.56	33.6655	63.2644	1879.20
y	42.0333	33.8703	805.80	37.3331	40.0028	1071.51
z	31.964	92.6219	2897.69	30.6785	101.773	3317.39
r_x	5.9099	6.0498	58.6522	6.5483	8.8324	77.2812
r_y	4.1431	13.0491	180.4621	3.526	16.352	265.71
r_z	N/A	N/A	N/A	N/A	N/A	N/A

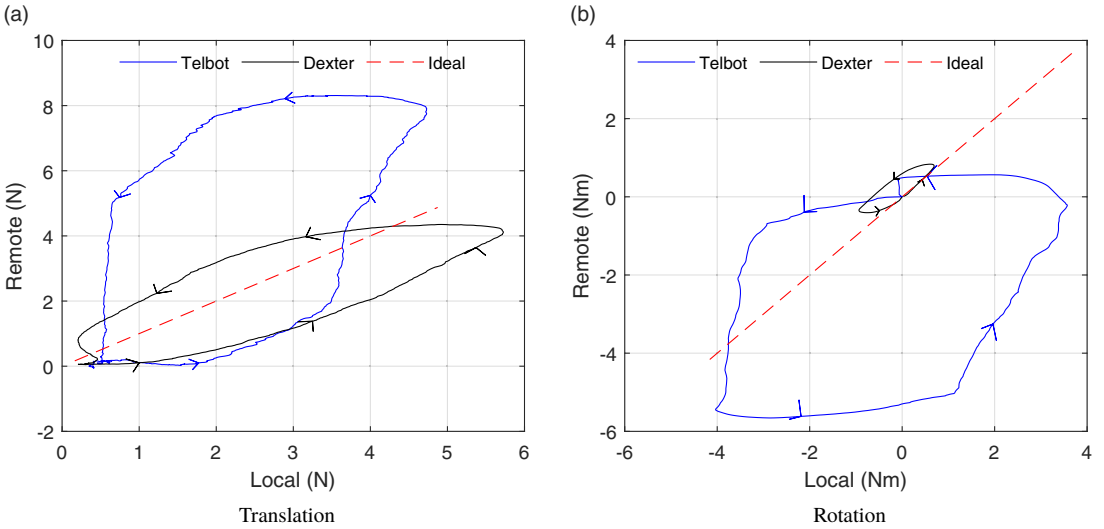


Figure 8. *Force transparency test conducted with Telbot and Dexter manipulators on both arms (LHS and RHS) across all translational and rotational axes. Left: translational axes; right: rotational axes.*

values are much lower at 0.4812 N and 1.6475 N, respectively. These findings suggest that Telbot may be more suitable for tasks requiring higher translational stiffness and resistance to displacement.

The effort sensitivity of both bilateral telerobotic systems for translation and rotation axes is depicted in Figure 8. The hysteresis curve in Dexter is relatively lower compared to that in Telbot.

3.2. Stiffness results

During the tests, FT measurements were taken on the local side, while displacements were recorded on both the local and remote sides. Stiffness values for both the Telbot and Dexter are provided in Tables III and IV, respectively. Higher stiffness values indicate increased rigidity in the corresponding axes. Typically, in the base frame, forward/backward (x) and upward/downward (z) stiffness values are relatively higher compared to side stiffness. The utilization of a gear-driven system on the remote side affects stiffness performance, and the Telbot system demonstrates notably higher stiffness values across all directions, particularly in the z-axis, with stiffness values reaching 2897.69 N m^{-1} on the LHS and 3317.39 N m^{-1} on the RHS. Dexter's stiffness values in the same axis are considerably lower, indicating reduced resistance to vertical deflection. This implies that the Telbot system is better equipped

https://doi.org/10.1017/S0263574724001826 Published online by Cambridge University Press

Table IV. *Stiffness (N m^{-1} – N m rad^{-1}) of the Dexter system in both arms.*

	Left Hand Side (LHS)			Right Hand Side (RHS)		
Direction	**Displacement (mm-deg)**	**Effort (N-N m)**	**Stiffness**	**Displacement (mm-deg)**	**Effort (N-N m)**	**Stiffness**
x	49.4459	16.8583	340.9439	49.4823	16.8212	339.9475
y	48.679	14.2995	293.751	49.4956	15.0483	304.034
z	48.1913	25.2615	524.1923	49.4988	26.3672	532.6827
r_x	19.9101	2.7833	8.0094	19.9944	2.4172	6.9266
r_y	19.9544	14.3444	41.1875	19.9945	11.9613	34.2761
r_z	19.9706	3.0081	8.6303	19.988	3.1439	9.012

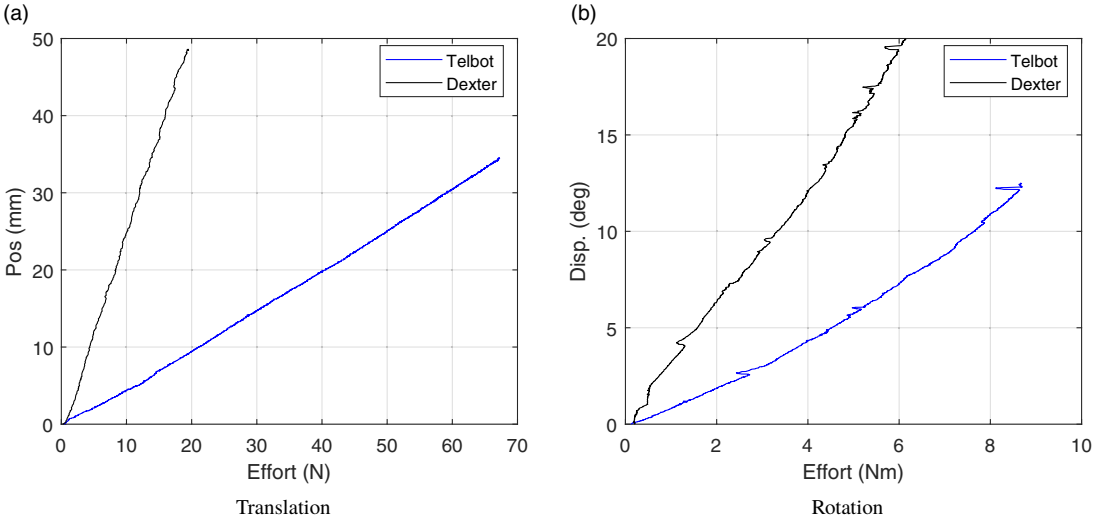


Figure 9. *Stiffness tests conducted with Telbot and Dexter manipulators on both arms (LHS and RHS) across all translational and rotational axes. Left: translational axes; right: rotational axes.*

to handle forces and torques with minimal deformation, especially in tasks involving vertical loads, see Figure 9.

Similar observation can be made on the rotational stiffness, Telbot has higher stiffness values in most directions, particularly in r_x and r_y. For instance, the r_y stiffness in Telbot is 180.4621 N m rad^{-1} on the LHS, whereas Dexter exhibits lower stiffness at 41.1875 N m rad^{-1}. These differences may influence the system's ability to handle rotational movements without excessive deflection. Stiffness testing could not be conducted for one rotation axis (r_z) with Telbot due to limitations in the torque of the motorized stages (the use of 'N/A' appropriately signifies instances).

3.3. Backdrivability results

To conduct backdrivability tests, motorized stages were mounted on the remote manipulators near the TCP (see Figure 6), and the actuators were operated while the local arm was in free space. The mechanical design of the Telbot remote arms, which incorporates gears from the base to the TCP for radiation protection, suggests that the system is not backdrivable. This characteristic is evident in Figure 10, where an application of approximately 200 N from the remote side is necessary to move both remote and local arms around 15 mm. The conducted test specifically focused on the z-axis to prevent any potential

https://doi.org/10.1017/S0263574724001826 Published online by Cambridge University Press

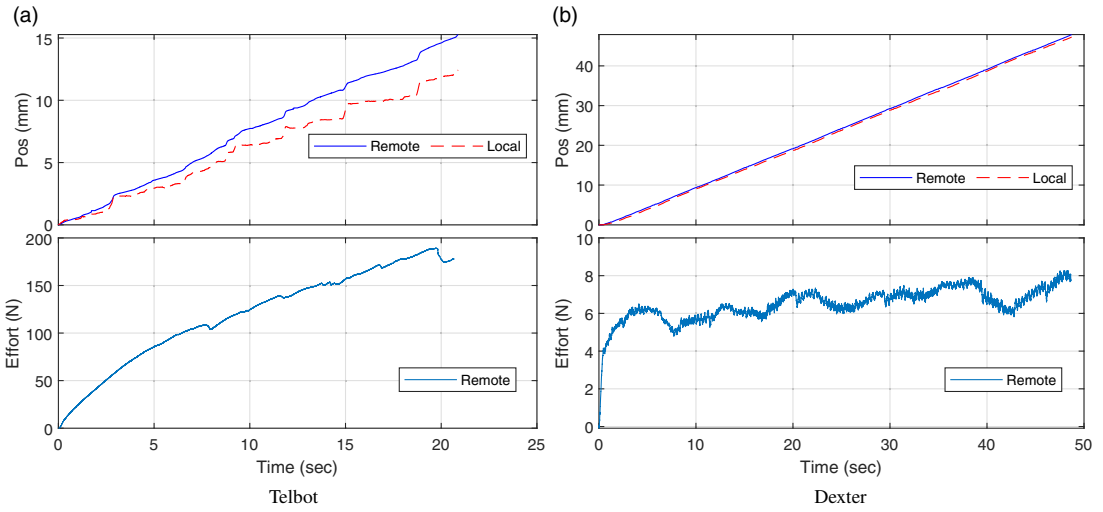


Figure 10. *Positions of TCP and handle with remote efforts during the backdrivability test in the z axis. Left: illustrating that Telbot is not backdrivable. Right: demonstrating that Dexter is backdrivable.*

damage to the robotic system. In contrast, Dexter is backdrivable as seen in Figure 10, where the remote manipulator is easily manipulated via the motorized stages with 5 N of effort, and the local manipulator closely follows the position of the remote manipulator.

4. Discussion

In addition to the performance criteria mentioned earlier, we also stress the systems to their operational limits to observe their behavior when operating beyond design boundaries. This is crucial for overall safety, as it ensures that the systems do not enter limit cycles–persistent oscillations with fixed amplitude and frequency. Such oscillations or vibrations may occur when the local manipulator is pushed close to its operational limits, such as when external forces are applied near maximum levels. One can state that both systems can be pushed to their limits without compromising safety, as no limit cycles were observed.

Effort transparency emerges as a pivotal performance criterion, although not explicitly specified by the manufacturer. These systems are primarily designed to transmit remote side efforts to the local side, enabling operators to execute precise manipulations without hardware and tool damage. The Dexter and Telbot performed well in force transparency, where approximately 1 N and 4 N from the local side are sufficient to transmit effort to the remote side, respectively. In free space, Dexter is highly transparent, requiring operators to apply only about 5 N. However, with Telbot, operators need to apply approximately 20 N, equivalent to handling around 2 kg during operations. This unintended impedance can contribute to fatigue during prolonged operations, and operators may find it challenging to distinguish efforts at the remote side less than 25 N (approximately 2.5 kg).

In any teleoperation system, whether uni- or bilateral, the primary performance requirement is the position tracking of the remote manipulator, where it is expected that the remote replicates the position displacement of the local manipulator. Although the accuracy is not reported here due to the lack of high-precision position measurement sensors, the representation of position displacement on the remote side is crucial. During the tests, it was observed that the position tracking of the remote Telbot manipulator contains discrete jumps (approximately 2 mm at the TCP) while tracking the position of the local arm, as shown in Figure 11 (a) (refer to Figure 11 (b) for the Dexter as a comparison). This nonlinear positional displacement is noticeable to the operators and can be attributed to the mechanical design of the telerobotic system, which includes various gears.

https://doi.org/10.1017/S0263574724001826 Published online by Cambridge University Press

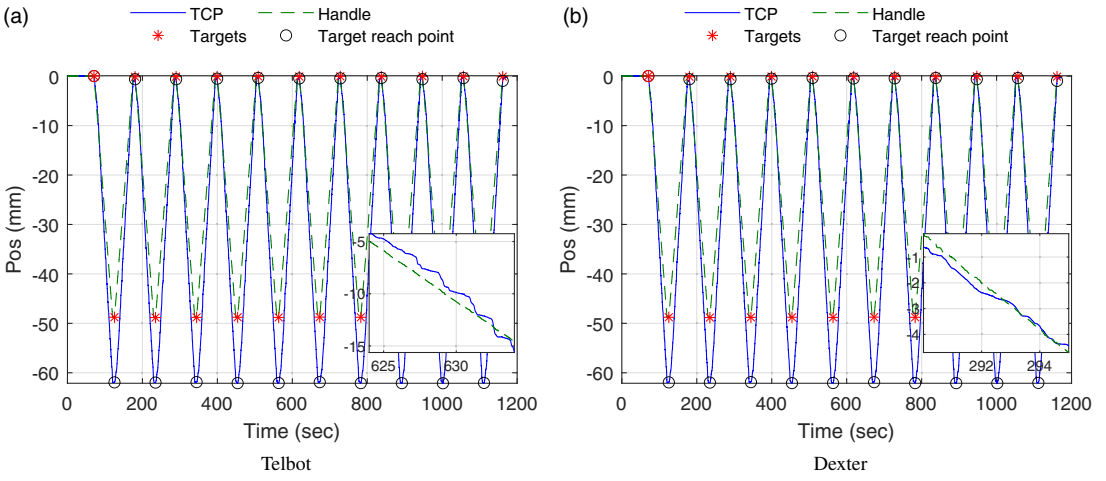


Figure 11. *Positions of the handle and TCP while the remote arm is in free space and the local arm is manipulated by the motorized stages in the z-direction. Left: Telbot including close-up view of the TCP motion containing discreet jumps. Right: Dexter's for comparison.*

4.1. Potential limitations

While every effort was made to mitigate some limitations (e.g., sensor and actuator limitations, mechanical rigidities and communication constraints), some inherent constraints in both the mechanical setup and the electrical systems may still influence the results. For example, slight mechanical deflections, sensor drift, and real-world communication latency might not be fully eliminated, despite our careful design and setup. These factors should be kept in mind when interpreting the experimental results, and further refinements in both hardware and testing conditions may be necessary for future work to reduce these limitations further.

5. Conclusion

In this article, we conducted a thorough evaluation of the performance of bilateral telerobotic systems, using the Telbot and Dexter dual-hand systems as case studies. We specifically examined the performances of the LHS and RHS systems, two distinct entities sharing the HMI for operational purposes. Alongside presenting measured performances, we detailed the test methodology and experiment procedures to standardize the evaluation of bilateral telerobotic systems. These operational capabilities provided crucial insights into their limitations, particularly important in scenarios such as nuclear operations where remote robustness is paramount.

Position tracking serves as a quantitative measure of performance; however, we acknowledged that in human-operated systems, operators may prioritize the manner in which motions are transmitted. They may prefer a linear, smooth transition over a non-linear hysteresis pattern. For a more comprehensive evaluation, future research will expand on performance metrics such as position accuracy and repeatability. Additionally, qualitative psychophysical tests via an operator study will provide a better understanding of human–robot interaction preferences, contributing to the design of more efficient and intuitive telerobotic systems.

In addition to evaluating the Telbot and Dexter systems, this study sets the stage for future work on standardizing the evaluation of bilateral telerobotic systems. By outlining a replicable methodology, we aim to contribute to the growing efforts to unify testing and operational metrics in this emerging field, ultimately benefiting the entire value chain—from design engineers to end users.

https://doi.org/10.1017/S0263574724001826 Published online by Cambridge University Press

Author contributions. HT, FA, MS, SS, WL, HMR, and KZ conceived and designed the study. HT, FA, MS, and SS performed the experimental testing and data collection. HT, FA, and WL conducted the data analysis, and HT wrote the article. IC and RS participated in proofreading.

Financial support. This research was fully funded within the LongOps program by UKRI under the Project Reference 107463, NDA, and TEPCO. The views and opinions expressed herein do not necessarily reflect those of the organizations.

Competing interests. The authors declare no conflicts of interest exist.

Ethical approval. Not applicable.

References

[1] A. Gani, O. Pickering, C. Ellis, O. Sabri and P. Pucher, "Impact of haptic feedback on surgical training outcomes: A randomised controlled trial of haptic versus non-haptic immersive virtual reality training," *Ann. Med. Surg.* **83**, 104734 (2022).
[2] J. Louca, K. Eder, J. Vrublevskis and A. Tzemanaki, "Impact of haptic feedback in high latency teleoperation for space applications," *ACM Trans. Human-Robot Interact.* **13**(2), 1–21 (2024).
[3] K. Darvish, L. Penco, J. Ramos, R. Cisneros, J. Pratt, E. Yoshida, S. Ivaldi and D. Pucci, "Teleoperation of humanoid robots: A survey," *IEEE Trans. Robot.* **39**(3), 1706–1727 (2023).
[4] J. Zhang, X. Zhang, Y. Cheng, Y. Cheng, Q. Zhang and K. Lu, "Nonlinear model predictive control (NMPC) based shared autonomy for bilateral teleoperation in CFETR remote handling," *Nucl. Eng. Technol.* **56**(10), 4437–4445 (2024).
[5] H. Tugal, J. Carrasco, P. Falcon and A. Barreiro, "Stability analysis of bilateral teleoperation with bounded and monotone environments via Zames-Falb multipliers," *IEEE Trans. Ctrl. Syst. Technol.* **25**(4), 1331–1344 (2016).
[6] B. Banks, M. Salehizadeh, A. Munawar, R. H. Taylor and U. Tumerdem, "Admittance switching for stability and transparency in human-robot collaborative microsurgery," *IEEE Robot. Autom. Lett.* **9**(2), 1891–1898 (2024).
[7] D. Duan, Y. Li and H. Li, "Factors affecting trust in the transparency index for stable and intuitive physical human-robot cooperation," *Trans. Inst. Meas. Ctrl.* **46**(8),1563–1578 (2024).
[8] R. Beerens, D. Heck, A. Saccon and H. Nijmeijer, "The effect of controller design on delayed bilateral teleoperation performance: An experimental comparison," *IEEE Trans. Ctrl. Syst. Technol.* **28**(5), 1727–1740 (2020).
[9] A. Heidari, N. J. Navimipour and A. Otsuki, "Cloud-Based Non-Destructive Characterization," **In:** *Non-Destructive Material Characterization Methods* (Elsevier, 2024) pp. 727–765.
[10] A. Heidari, N. J. Navimipour and M. Unal, "Applications of ML/DL in the management of smart cities and societies based on new trends in information technologies: A systematic literature review," *Sustain. Cities Soc.* **85**, 104089 (2022).
[11] E. Samur, *Performance Metrics for Haptic Interfaces* (Springer Science & Business Media, 2012).
[12] D. Buongiorno, D. Chiaradia, S. Marcheschi, M. Solazzi and A. Frisoli, "Multi-dofs exoskeleton-based bilateral teleoperation with the time-domain passivity approach," *Robotica* **37**(9), 1641–1662 (2019).
[13] T. L. Brooks, "Telerobotic Response Requirements," **In:** *IEEE international conference on systems, man, and cybernetics* (1990) pp. 113–120.
[14] M. Uebel, M. Ali and I. Minis, "The effect of bandwidth on telerobot system performance," *IEEE Trans. Syst. Man Cybern.* **24**(2), 342–348 (1994).
[15] V. Hayward and O. R. Astley, "Performance Measures for Haptic Interfaces," **In:** *Robotics research: The seventh international symposium*, London, Springer (1996) pp. 195–206.
[16] M. C. Çavuşoğlu, D. Feygin and F. Tendick, "A critical study of the mechanical and electrical properties of the phantom haptic interface and improvements for highperformance control," *Presence: Teleoperators and Virtual Environ.* **11**(6), 555–568 (2002).
[17] B. Taati, A. M. Tahmasebi and K. Hashtrudi-Zaad, "Experimental identification and analysis of the dynamics of a PHANToM premium 1.5A haptic device," *Presence: Teleoperators and Virtual Environ.* **17**(4), 327–343 (2008).
[18] H. Li and K. Kawashima, "Experimental comparison of backdrivability for time-delayed telerobotics," *Ctrl. Eng. Pract.* **28**, 90–96 (2014).
[19] Y. Deng, Y. Tang, B. Yang, W. Zheng, S. Liu and C. Liu, "A Review of Bilateral Teleoperation Control Strategies with Soft Environment," **In:** *6th IEEE International Conference on Advanced Robotics and Mechatronics, ICARM* (2021) pp. 459–464.
[20] S. N. F. Nahri, S. Du and B. J. Van Wyk, "A review on haptic bilateral teleoperation systems," *J. Intell. Robot. Syst.* **104**(1), 13 (2021).
[21] I. Görgülü, M. I. C. Dede and G. Carbone, "Experimental structural stiffness analysis of a surgical haptic master device manipulator," *J. Med. Devices* **15**(1), 011110 (2021).
[22] P. Malysz and S. Sirouspour, "Nonlinear and filtered force/position mappings in bilateral teleoperation with application to enhanced stiffness discrimination," *IEEE Trans. Robot.* **25**(5), 1134–1149 (2009).
[23] G. A. Pratt, M. M. Williamson, P. Dillworth, J. Pratt and A. Wright, "Stiffness isn't Everything," **In:** *Experimental Robotics IV: The 4th International Symposium*, California, Berlin Heidelberg, Stanford, Springer (1997) pp. 253–262.

https://doi.org/10.1017/S0263574724001826 Published online by Cambridge University Press

[24] S. E. Salcudean and T. D. Vlaar, "On the emulation of stiff walls and static friction with a magnetically levitated input/output device," *J. Dyn. Sys. Measure. Ctrl.* **119**(1), 127–132 (1997).
[25] R. Skilton, N. Hamilton, R. Howell, C. Lamb and J. Rodriguez, "MASCOT 6: Achieving high dexterity tele-manipulation with a modern architectural design for fusion remote maintenance," *Fusion Eng. Des.* **136**, 575–578 (2018).
[26] R. Chu, Y. Zhang, H. Zhang, W. Xu, J. H. Ryu and D. Wang, "Co-actuation: A method for achieving high stiffness and low inertia for haptic devices," *IEEE Trans. Hapt.* **13**(2), 312–324 (2020).
[27] L. A. Jones and I. W. Hunter, "A perceptual analysis of stiffness," *Exp. Brain. Res.* **79**(1), 150–156 (1990).
[28] F. Gosselin, F. Ferlay and A. Janot, "Development of a new backdrivable actuator for haptic interfaces and collaborative robots," *Actuators* **5**(2), 17 (2016).
[29] H. Li, W. Liu, K. Wang, K. Kawashima and E. Magid, "A cable-pulley transmission mechanism for surgical robot with backdrivable capability," *Robot. Comput.-Integr. Manuf.* **49**, 328–334 (2018).
[30] W. Wälischmiller and H.-Y. Lee, *Development and Application of the Telbot System* (Springer, Vienna, 1997) pp. 399–408.
[31] International Organization for Standardization 1998. *Manipulating Industrial Robots - Performance Criteria and Related Test Methods Technical Report*, *ISO*.
[32] G. Carbone, "Stiffness Analysis for Grasping Tasks," **In:** *Grasping in Robotics* (Springer, London, 2013) pp. 17–55.
[33] D. C. Lin, C. P. McGowan, K. P. Blum and L. H. Ting, "Yank: The time derivative of force is an important biomechanical variable in sensorimotor systems," *J. Exp. Biol.* **222**(18), (2019).
[34] A. Klimchik, A. Pashkevich and D. Chablat, "Fundamentals of manipulator stiffness modeling using matrix structural analysis," *Mech. Mach. Theory* **133**, 365–394 (2019).

Cite this article: H. Tugal, F. Abe, M. Sakamoto, S. Shirai, I. Caliskanelli, W. Liu, H. Marin-Reyes, K. Zhang and R. Skilton (2025). "Nuclear bilateral telerobotic systems: performance comparison and future implications", Robotica **43**, 242–255. https://doi.org/10.1017/S0263574724001826

https://doi.org/10.1017/S0263574724001826 Published online by Cambridge University Press